Construction and Building Materials 372 (2023) 130821

Contents lists available at ScienceDirect

Construction and Building Materials

journal homepage: www.elsevier.com/locate/conbuildmat

Heat-induced explosive spalling of self-prestressing, self-compacting concrete slabs

Hussein Mohammed [a,c,*], Fariza Sultangaliyeva [b], Mateusz Wyrzykowski [c], Giovanni Pietro Terrasi [c], Luke Bisby [a]

[a] School of Engineering, The University of Edinburgh, UK
[b] Université de Pau et des Pays de l'Adour, E2S UPPA, SIAME, Anglet, France
[c] Empa, Swiss Federal Laboratories for Materials Science and Technology, Switzerland

ARTICLE INFO

Keywords:
Heat-induced spalling
Self-prestressing
CFRP
Simulated ISO 834
Moisture content
Self-compacting concrete

ABSTRACT

A novel concrete mix has been developed that can achieve high levels of self-prestressing through the controlled expansion of the concrete sample with cast-in carbon fibre reinforced polymer (CFRP) bars. Experiments have shown that the mechanical properties and durability of the mix are not adversely affected by the mix's self-expanding nature. However, the behaviour of this mix at elevated temperatures is largely unknown, raising legitimate concerns regarding the fire performance of the resulting self-prestressed concrete elements. The research presented in this paper investigates the behaviour of concrete elements manufactured from self-prestressed, self-compacting concrete (SPSCC) when exposed to severe heating – such as would likely be experienced during a building fire. Nine specimens, with dimensions (600 mm × 200 mm × 45 mm) were tested under one-sided exposure to an experimentally simulated ISO 834 standard heating regime. The results showed that the SPSCC samples were acutely prone to explosive spalling under these conditions. The results also suggest that the comparatively higher moisture content of SPSCC samples, as compared with conventional concrete mixes of similar composition and mechanical properties, appeared to be the most critical factor for heat-induced concrete cover spalling. Higher prestress (compressive) forces also appeared to exacerbate the spalling likelihood of SPSCC samples. The addition of 2 kg/m^3 of polypropylene (PP) fibres led to the complete elimination of spalling in SPSCC samples. The self-prestress levels in samples with PP fibres were 30 % less than those without PP fibres, for reasons which require additional investigation. Differential thermal expansion between the internal CFRP bars and the concrete was observed to restrain the elongation and thermal curvature of the samples during heating, up until the point where the bars debonded from the surrounding concrete due to elevated temperature and (presumed) increased tensile stress in the tendon anchorage zones. The results provide compelling evidence supporting the need to include PP fibres within high-performance, self-prestressing, self-compacting concrete slabs.

1. Introduction

Prestressed concrete has been widely used in the construction sector for decades. There are many advantages to prestressed concrete as compared with reinforced concrete, with the main benefits being a reduction in tension cracking, superior control of deflections, and more effective utilisation of resources [1]. Prestressed concrete can be further categorised into pre-tensioned and post-tensioned construction, based on the manner with which the tensioning of the prestressing bars occurs (i.e., prior to pouring of the concrete or afterwards). Regardless of the method used, inducing prestress is a process that requires skilled labour, introduces significant construction hazards, and is resource heavy; all of which have the potential to make prestressed concrete less attractive in the construction industry despite its clear functionality and sustainability benefits.

A novel method of achieving comparable prestress levels to those achieved via traditional methods, and that simplifies casting and prestressing operations, has recently been developed at Empa [2]. The process uses a concrete mix that experiences controlled expansion during initial curing, with embedded, bonded, ultra-high modulus (UHM)

* Corresponding author at: School of Engineering, The University of Edinburgh, UK.
E-mail address: Hussein.Mohammed@ed.ac.uk (H. Mohammed).

https://doi.org/10.1016/j.conbuildmat.2023.130821
Received 13 December 2022; Received in revised form 17 February 2023; Accepted 19 February 2023
Available online 1 March 2023

carbon fibre reinforced polymer (CFRP) bars (Modulus of Elasticity E_{11} = 502 GPa). Pretension is induced in the CFRP bars in the early stages of curing via a tailored, controlled expansion of the concrete. Thus, the bulk of the work associated with pretensioning of the bars, as well as the health and safety hazards associated with these activities, are eliminated. The self-prestressed, self-compacting concrete (SPSCC) mix and methodology are reported in detail elsewhere [2,3].

Due to the novelty of this type of self-prestressed concrete mix, research regarding its behaviour in fire is extremely limited. Preliminary research [4] suggested that SPSCC concrete planks (i.e. thin slabs) are prone to severe heat-induced spalling when subjected to steep internal thermal gradients (such as generated under exposure to fire).

One of the critically important components of the novel SPSCC mix design is superabsorbent polymer (SAP). SAP particles can absorb several times (more than 15 times) their mass in moisture during mixing, without becoming dissolved. Therefore, SAP is used as way to mitigate self-desiccation and autogenous shrinkage for the concrete on curing by gradually releasing, over time, the moisture that it absorbs during mixing and casting [5]. However, the water absorbed by the SAP leads to an increased proportion of effectively free moisture within the concrete. Given the widely accepted observation that concretes with higher moisture contents are more prone to heat-induced explosive concrete cover spalling [6,7], the higher pore moisture content resulting from SAP addition is likely to affect the spalling propensity of SPSCC mixes. However, research [8] has also shown the potential positive effects of a combination of SAP and polypropylene (PP) fibres, when used together, in preventing heat induced spalling [8]; this was hypothesized as being the result of a higher interconnectivity of microcracks once the SAP particles are void of water.

To explore some of the issues highlighted above, this paper investigates the behaviour of SPSCC concrete planks under extreme fire loading. The influencing parameters governing the spalling behaviour of such planks, along with ways to mitigate such behaviour are considered; this includes the addition of polypropylene fibres (PP), which have been shown to be very effective in reducing (even eliminating) heat induced spalling. This paper also considers the effects of drying of samples on the propensity of concrete planks to spall; and further work is recommended.

2. Methods

2.1. Sample preparation

In total, 9 concrete planks were fabricated using three mixes (three specimens per mix). Each specimen contained two bars that were made of either UHM CFRP or high strength steel (see Table 1). The first mix (Ref) was a control mix used as a benchmark. The second mix (PP) included 2 kg/m^3 of PP microfibres, but otherwise identical to the control mix. The PP fibres were 18 mm long, and the diameter was 34 μm (on average). The melting temperature for the PP fibres (as provided by the supplier) was in the range of 150–170 °C. The third concrete mix (St) was identical to the control mix but was cast with steel bars instead of CFRP bars. This was done primarily to investigate the effects of reduced prestressing on spalling, given the lower modulus of elasticity for the steel bars. The steel bars used had an elastic modulus (E_{11}) of 205 GPa, compared to the higher modulus of elasticity for the CFRP bars of 502 GPa. Details of the reinforcing bars are given in Table 1.

The naming of the samples is based on the mix and the type of internal reinforcement used; Ref-CFRP indicates refers to samples made using the Ref mix with CFRP bars, Ref-Steel indicates that the samples were made using the Ref mix with steel bars, and PP-CFRP means the samples were made using the PP mix and CFRP bars. Letters A, B, and C are used to identify the samples in each series.

Table 1
Details of the reinforcing bars used in the current study.

Bar Type	Diameter (mm)	E_{11}	Remarks
CFRP	5.4	502	Sand-coated
Steel	6.0	205	Ribbed

The calcium-sulfoaluminate (CSA), which is the expansive agent, had the following composition (determined using Rietveld analysis): anhydrite 48 %, ye'elimite 22 %, lime 19 %, portlandite 9 %, periclase 1 %, calcite 1 %. The Blaine fineness of the CSA additive was 0.36 m^2/g and the density was 2.91 g/cm^3. The rest of the dry materials used for the mix design have been reported fully in previous publications [2,5], and are not repeated here.

The mix composition that was used for each of the 3 batches was identical, except for the differences mentioned above. Table 2 provides a detailed mix composition.

The dry materials were first mixed in a rotating mixer for two minutes. The superplasticiser and the SRA were added to the water, which was then added to the dry mix. For the second mix (PP), the fibres were added after the addition of the water, and mixed for a further two minutes.

The fresh concrete was poured into moulds with inner dimensions (200 mm × 600 mm × 45 mm). Cylindrical moisture content samples (55 mm high, 55 mm in diameter) were also produced to measure the concrete moisture content at the time of fire testing. 6 pieces of 160 mm × 40 mm × 40 mm unreinforced concrete prisms were also produced to determine the modulus of elasticity and the compressive strength of the mixes at 28 and 222 days. The geometry of the samples is shown in Figs. 1 and 2.

A thermocouple (TC) array was inserted into the concrete planks during casting to enable in-depth temperature measurement during the spalling experiments (at 2, 10, and 22.5 mm from the heat-exposed surface). A further TC was attached to the side of one of the prestressing bars at the centre of the concrete plank (i.e., 22.5 mm from the heat-exposed surface).

During the experiments, two further TCs were used; one was attached to the centre of the exposed front of the specimen, and the other to the centre of the unexposed face of the sample.

2.2. Curing

The samples were covered with a polyethylene sheet after casting, and demoulded after 20 h. After demoulding, the samples were transferred to a water bath maintained at 20 °C. The samples were removed from the water bath after 28 days and transferred to a climate-controlled chamber at 20 °C and 56 % relative humidity (RH). The samples were removed from the climate chamber after 78 days, and were kept in wooden crates, in an uncontrolled laboratory space (at 5–15 °C and 60–70 % RH) until they were tested. Shipment of the samples from Empa to the University of Edinburgh (where the spalling experiments were carried out) took 4 days during the European spring season, during which time the environmental conditions were unknown.

Table 2
Mix proportion for the concrete casts presented in the current study.

Material	Quantity (Reference mix)	Quantity (PP mix)
Cement CEM I 52.5R (kg/m^3)	491	491
Aggregates (0–8 mm) (kg/m^3)	1486	1486
SAP (kg/m^3)	2.76	2.76
Limestone powder (kg/m^3)	24.6	24.6
Shrinkage reducing admixture (SRA) (kg/m^3)	14.9	14.9
Superplasticiser (% of cement)	1.3 %	1.3 %
Water (kg/m^3)	223	223
Calcium-sulfoaluminate cement or CSA cement (kg/m^3)	78.6	78.6
PP fibres (kg/m^3)	–	2
Spread (mm)	745	575

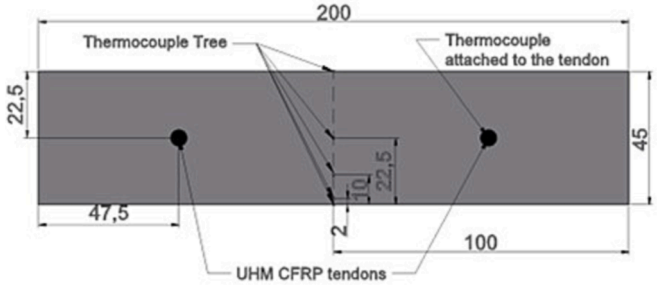

Fig. 1. Cross section of the planks.

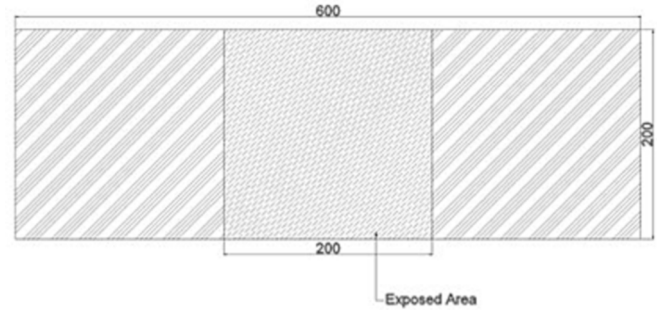

Fig. 2. Front elevation view of the samples, with the heated area highlighted.

2.3. Prestress development

The development of prestressing in the samples (induced by the presence of UHM CFRP bars and the expansion of the concrete) was recorded by resistive linear strain gauges (Type HBM SG250, gauge length 6 mm). The strain gauges were bonded to the middle of the prestressing bars prior to the casting of the samples. Each sample was equipped with a minimum of two strain gauges (one on each tendon). The bonding of the strain gauges to the bars is shown in Figs. 3 and 4. The tendon was first cleaned, and the strain gauges were bonded to the bars using a fast action glue (HBM Z 70). The gauges were then covered with three layers of protection to guard against chemical/mechanical damage during casting and testing. First, a layer of HBM P 140 was used, and after 24 h a second layer of protective silicon (HBM SG 250) was added. After a further 7 days, a final layer (HBM AK 22) was applied.

Despite the small size of the strain gauges, the protective layers had to be applied over a relatively large area to ensure adequate protection to the gauges. The resulting, measured development of prestress (based on strain measurements) with time is shown in Figs. 5 through 7.

The prestress development within the concrete planks and the variation amongst the three series of samples is discussed in the self-prestress development section below (see Fig. 6).

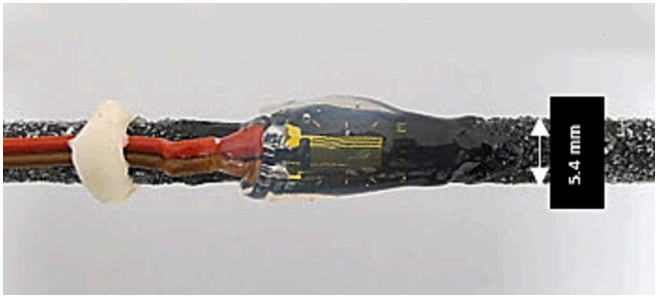

Fig. 3. CFRP tendon with HBM SG 250 applied.

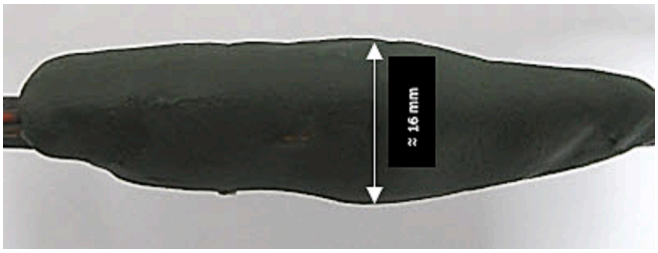

Fig. 4. CFRP tendon with all the protective layers applied.

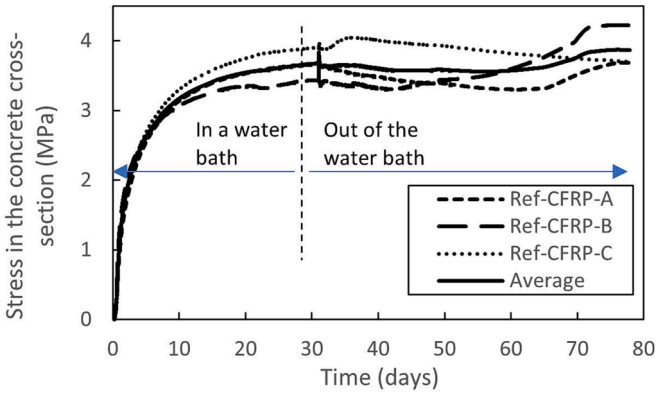

Fig. 5. Prestress development in Ref-CFRP samples.

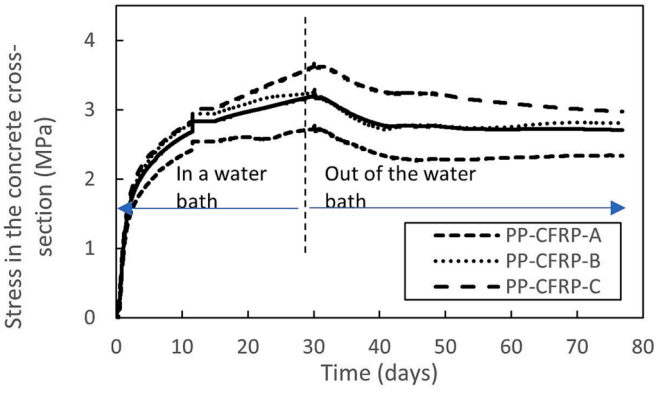

Fig. 6. Prestress development in PP-CFRP samples.

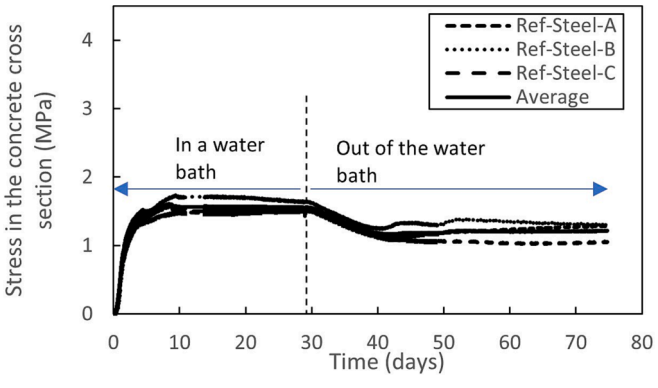

Fig. 7. Prestress development in Ref-Steel samples.

2.4. Mechanical properties at ambient temperature

The modulus of elasticity and the compressive strength of the samples were determined from tests on small prisms (160 mm × 40 mm × 40 mm) fabricated during the casting of the planks. A summary of the mechanical properties for each mix (at ambient temperature) is given in Table 3. The values shown in Table 3 are the average, and the standard deviation (SD) is given in brackets.

2.5. Test set up

A mobile, gas-fired radiant panel array (RPA) was used for the spalling experiments. The working principles of the RPA are reported elsewhere [9–11]. The concrete planks were positioned horizontally (as shown in Figs. 2 and 9) and were tested in a mechanically unrestrained condition (i.e., the samples were free to thermally expand on heating). The central section of the sample, with a surface area of 200 mm × 200 mm, was exposed to an incident heat flux (q''). This was achieved using a 200 mm × 200 mm opening within a thermally-insulating vermiculite board that shielded the displacement instrumentation behind. The test set up is shown in Fig. 8.

Thermal bowing of the specimens on heating was measured during the experiments using three linear potentiometers (LP) that were attached to the cold side of the specimens (Fig. 9). Further LPs were attached to both ends of the specimen (Fig. 10) to monitor the elongation of the sample (in-plane) and the draw-in (or slip) of the prestressing bars upon debonding.

The mobile RPA was used to produce in-depth heating equivalent to that which would be experienced under exposure to an ISO 834 standard fire curve. The details of the validation of this approach is outlined elsewhere [4,9].

Fig. 11 shows a schematic of the out-of-plane curvature (i.e., thermal bowing) of the concrete planks when heated.

The total magnitude of the thermal bowing (shown in Fig. 11 as 'Delta') was calculated as the sum of the bowing at the centre of the plank (measured as Delta 1) and the average of the reverse movements of the plank at its edges (Delta 2 and Delta 3).

2.6. Testing matrix

The samples were all subjected to the simulated ISO 834 heating exposure for a duration of 60 min. However, for the samples that spalled the test was terminated after the main spalling event occurred, so as to avoid damaging the RPA. Table 4 shows the details of the testing matrix. The moisture content of the samples was determined by placing small cylindrical samples in an oven at 105 °C, and measuring the weight loss between 24 h intervals. Drying continued until the difference between two consecutive measurements (24 h apart) was less than 0.1 % of the dried weight of the sample.

All the samples were aged more than six months when tested, except for Ref-CFRP-A, which was five months old at the time of testing. Furthermore, Ref-CFRP-C was air dried in an oven (at 80 °C) prior to the experiments. The drying was continued until the difference between two consecutive mass measurements (24 h apart) was less than 1 % of the sample's mass. This threshold was achieved after 7 days of drying. The sample was then left at ambient temperature (in the laboratory where the test took place) until the temperature at its centre reached 30 °C (measured with a TC that was installed during casting).

Table 3
Mechanical properties of the mixes at ambient temperature.

Mix	E_{11} (MPa) (28 days) (SD)	Compressive strength (MPa) (28 days) (SD)	E_{11} (MPa) (180 days) (SD)	Compressive strength (MPa) (222 days) (SD)
Ref	20.5 (0.1)	52.1 (3.75)	28.7 (0.1)	67 (4.28)
PP	21.6 (5.8)	53.6 (3.44)	27.6 (1.8)	65.4 (1.96)
St	20.5 (1.1)	54.9 (2.29)	24.6 (2.8)	60.4 (3.27)

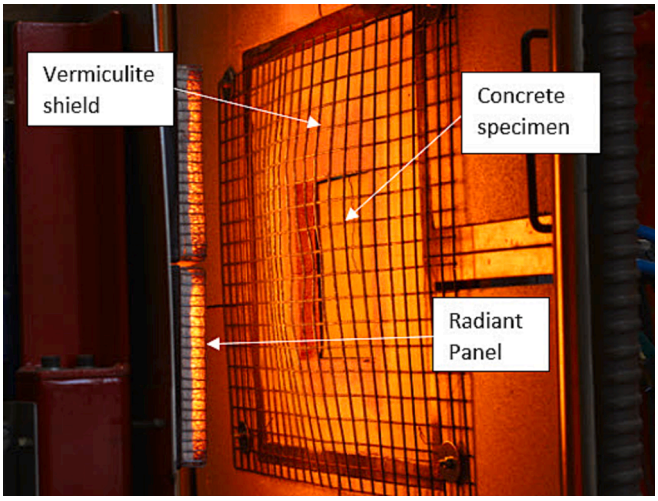

Fig. 8. Test set up comprising the RPA and the vermiculite shield.

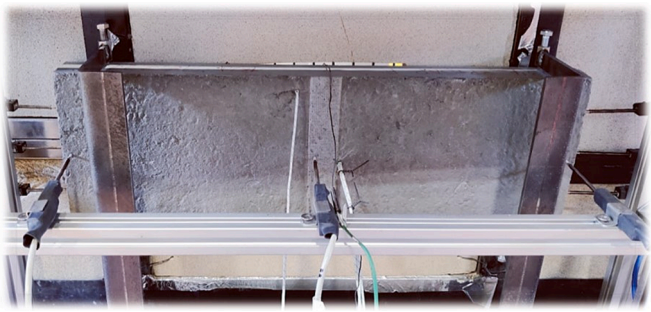

Fig. 9. LPs measuring thermal bowing.

2.7. Experimental results

The results from the spalling experiments are outlined in Table 4. Both samples Ref-CFRP-A and Ref-CFRP-B spalled early. Specimen Ref-CFRP-A experienced one instance of violent spalling at 9 min and zero seconds (9′00″). specimen Ref-CFRP-B first spalled at 5′59″ and continued spalling until 10′00″ when the test was terminated. During the experiment on specimen Ref-CFRP-B, 8 instances of spalling, of differing severity, were recorded. Fig. 12 shows a still-frame image of the specimen Ref-CFRP-A at the moment of spalling, and Fig. 13 shows specimen Ref-CFRP-A after testing. These results are compatible with earlier experiments reported in [4].

The Ref-CFRP-C specimen (pre-dried at 80 °C for 7 days) did not spall, despite being subjected to the same heating regime as Ref-CFRP-A and Ref-CFRP-B samples. The CFRP prestressing bars in specimen Ref-CRFP-C slipped within the concrete at 18′45″ (the temperature at the tendon surface was 250 °C at the moment of slippage). Neither Ref-CFRP-A nor Ref-CFRP-B samples experienced any tendon slippage.

As for the specimens with steel bars (St), Sample Ref-Steel-A experienced one instance of explosive spalling similar to Sample Ref-CFRP-A. However, Sample Ref-Steel-A spalled at 14′56″ (almost six minutes later than Sample Ref-CFRP-A). The remaining two specimens belonging to this mix (i.e., samples Ref-Steel-B and Ref-Steel-C) did not spall. No reinforcement slippage was observed for the specimens with steel bars.

Specimens with 2 kg/m^3 of PP fibres completely avoided spalling. In the samples with PP fibres, the CFRP prestressing bars also avoided slippage. Similar to Ref-CFRP, the PP-CFRP samples all developed

Fig. 10. LPs measuring elongation.

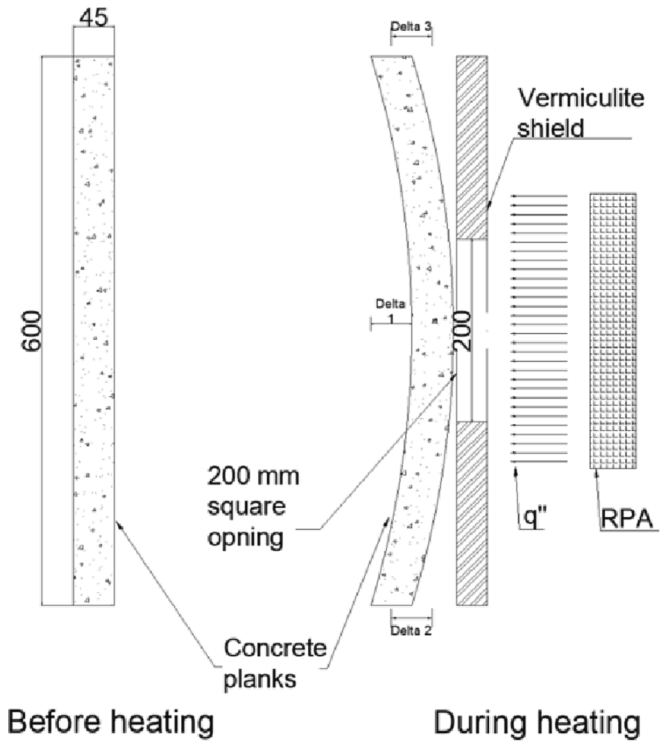

Fig. 11. Schematic of the thermal bowing (top view) of the horizontally positioned concrete planks.

longitudinal reflection cracks (in the concrete along the lines if the internal prestressing bars) on their unexposed surfaces. However, these cracks were comparatively less prominent (and narrower) than the cracks observed for Ref-CFRP-C, and were observed to form at a later stage or heating (see Fig. 19 and Table 5).

3. Discussion

3.1. Mechanical properties

The compressive strengths of the self-prestressed mixes were above 50 MPa and 60 MPa, at 28 days and 222 days, respectively (see Table 3). These strengths were lower than those reported in similar prior work [2,3]. The constituent materials used for the mixes were obtained from the same sources as the mixes reported in these references, however in the current study the amount of SAP was increased (refer to Table 2). The cement content for the mixes reported in the current study was also less than in prior work [2,3]. The inferior strength of the samples in the current work (as compared to those reported in prior work) can thus be explained by the additional SAP and the higher water/cement ratio. Previous studies have confirmed that larger proportions of SAP lead to lower compressive strengths, especially at earlier ages [5]. The results obtained in the current study are thus compatible with prior research.

The compressive strength of the specimens tested for this study shows the inadequacy of the current guidance provided in the Eurocode to mitigate spalling [12]. At present, spalling mitigation measures (through the addition of PP fibres) are recommended only when the concrete grade is higher than C80/95. The results from this study show that the mixes with lower compressive strength than what is outlined in the Eurocode are still susceptible to explosive spalling, and therefore require spalling mitigation. Further research has also confirmed the likelihood of low strength concrete to spall under severe heat conditions [13].

3.2. Self-prestress development

The time history of self-prestressing for the samples in the current study is shown in Figs. 5 through 7. These show that the samples experienced a small amount of shrinkage once they were taken out of the water bath at 28 days. This is particularly evident in the Ref-Steel samples and the PP-CFRP samples. The shrinkage continued for a period of around 10 days before the strain measurements then stabilised.

The final measured prestress levels (at 78 days after casting), inferred from strain gauge readings on the bars, show that self-prestressing in the PP mix was, on average, 30 % less than the prestress levels in the Ref mix. The available literature is not conclusive regarding the effects of PP fibre inclusion on the mechanical properties of concrete at ambient temperature; wherein some researchers have reported an increase in the tensile and flexural strength of PP fibre reinforced concrete [14,15,16] whilst others have not observed any measurable difference, or have even reported reductions in strength with the inclusion of PP fibres [17]. Arguments for the increased tensile strength are generally based on the idea that PP fibres may prevent the development of micro-cracks at an early stage of loading. However, once such cracks have formed, PP fibres (which have a comparatively low modulus) are unlikely to contribute towards additional strength. During the spalling tests reported herein, it was observed that specimens with PP fibres developed longitudinal cracks along the CFRP bars at a later stage of heating than sample Ref-CFRP-C, as shown in Table 5.

Table 5 five suggests that the addition of PP fibres may slow down crack propagation, which could at least partially explain the reduction in the amount of expansion for samples with PP fibres. However, drawing firm conclusions regarding the reason for less expansion in the PP mix

Table 4
Mechanical properties and the time-to-spalling for respective samples.

Mix	Type of Bar	Sample	Age (day)	Prestress (MPa)	Test Duration (min)	Tendon slip	Time to spall	Spalling depth (mm)	Moisture content % (at the time of test)
Ref	CFRP	A	150	3.69	9	No	9′00″	12.4	5.93
		B	184	4.22	10	No	5′59″	10.1	5.51
		C	188	3.7	60	Yes	NA	NA	2.46
PP	CFRP	A	192	2.34	60	Partial	NA	NA	5.12
		B	195	2.81	60	No	NA	NA	5.12
		C	196	2.97	60	No	NA	NA	5.12
Ref	Steel	A	190	1.28	15	No	14′56″	23.5	5.51
		B	190	1.3	60	No	NA	NA	5.51
		C	191	1.05	60	No	NA	NA	5.51

Fig. 12. Still frame of specimen Ref-CFRP-A with debris flying towards the RPA.

Fig. 13. Specimen Ref-CFRP-A after cooling down.

requires additional research.

The levels of prestress would have undoubtedly changed during spalling experiments. The changes in the prestress levels are due to the differential thermal expansion of the concrete and the CFRP, the deteriorating mechanical and bond properties of both the concrete and the prestressing bars embedded within it [18,19].

Table 5
Details of the time-to-cracking and tendon temperature at longitudinal reflective cracking for samples with CFRP bars.

Reference	PP-CFRP-A	PP-CFRP-B	PP-CFRP-C	Ref-CFRP-C
Time-to-Crack (minutes′ seconds″)	26′05″	23′47″	32′19″	10′48″
Temperature (°C)	245	224	308	157

3.3. Temperature profiles

Fig. 14 shows the in-depth temperature–time history for the first 10 min of the experiments on Ref-CFRP samples. All three samples show comparable in-depth temperatures, with the maximum difference being 18 °C in the 10th minute. The time history of the in-depth temperatures beyond the 10th minute are not shown because of the occurrence of spalling in samples Ref-CFRP-A and Ref-CFRP-B. No significant differences between the time–temperature history for any of the Ref samples was evident. Fig. 14 demonstrates that the pre-drying of specimen Ref-CFRP-C did not lead to obvious variance of heat transfer through the sample when compared against specimens Ref-CFRP-A and Ref-CFRP-B.

A comparison of the time–temperature history at the mid depth of the samples between Ref-CFRP-C and the samples which did not spall is presented in Fig. 15. This figure shows that Sample Ref-CFRP-C (which was pre-dried at 80 °C and thus also commences at a slightly higher initial temperature) differs from the other samples in that the temperature evolution at its mid depth fails to show a ‘kink’ at about 180 °C, thus suggesting that the kink is related to moisture transport and evaporation within the samples. The kink is thought to be due to the formation of a moving moisture saturated front (more commonly known as moisture clog).

Also evident in Fig. 15 is that there is a difference between the PP-CFRP and the Ref-CFRP samples in terms of the location of the kink. The PP-CFRP samples show a less acute kink when the temperature reaches about 170 °C. The Ref-Steel samples, on the other hand, show a more pronounced kink and at a higher temperature (ranging between 185 and 195 °C). This could be explained by the enhancement of moisture migration that occurs when PP fibres are used (i.e., higher rate of moisture migration into the deeper, colder regions of the heated concrete is made possible when PP fibres are used). Mcnamee et al. [20] reported observing a much more concentrated wet layer in samples that contained no PP compared to samples with 1 kg/m^3 of PP fibres (i.e., specimens with PP fibres showed evidence of moisture migration further into the colder regions of concrete compared to specimens without fibres). The more distinct kinks forming in non-fibre samples (Fig. 15) corroborate what was reported by Mcnamee et al. [20]. Researchers [21] have also observed that concrete samples with PP fibres experience rapid increases in gas permeability at temperatures below the melting point of the fibres; the increased permeability is thought to be explained

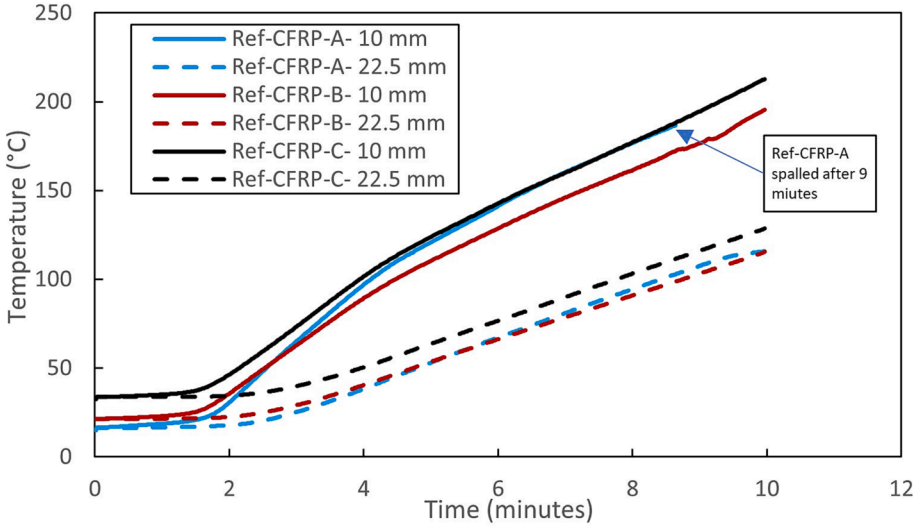

Fig. 14. In-depth temperatures (at 10 mm and 22.5 mm) recorded for samples Ref-CFRP-A to Ref-CFRP-C during heating.

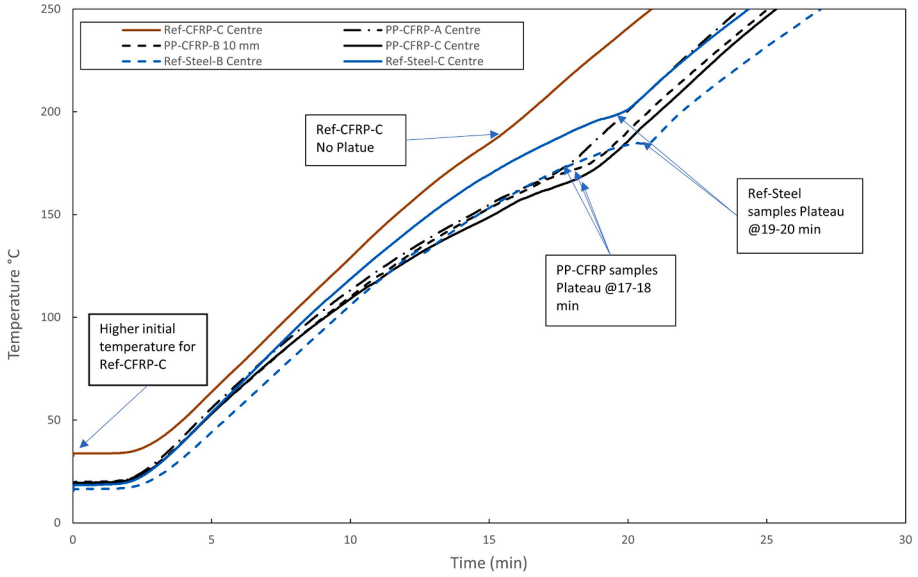

Fig. 15. Temperature-time history at the sample mid-depth for the self-prestressed samples that did not experience spalling.

by the formation of microcracks in the transition zone within the concrete matrix surrounding the fibres. The cracks are caused by a thermal mis-match between the fibres and the concrete [22] which better enables the migration of moisture driven by temperature gradients.

Apart from the differences already mentioned, there are no other significant differences in the measured in-depth temperatures when comparing Sample Ref-CFRP-C and the other samples.

3.4. Thermal bowing

Thermal bowing occurs in the heated plate samples because of differential thermal expansion through the specimens' thickness upon rapid heating, and when the specimens are mechanically unrestrained. The thermal bowing of both samples Ref-CFRP-B and Ref-CFRP-C from the current study is shown in Fig. 16. The time history of the thermal bowing for Sample Ref-CFRP-B is shown up to the 10th minute of the experiment (due to subsequent spalling). The thermal bowing of the samples appeared – unsurprisingly – to be strongly influenced by the type and behaviour (i.e., slippage or otherwise) of the prestressing bars. Samples with CFRP bars (i.e., Ref-CFRP, PP-CFRP) showed greater resistance to overall elongation than samples with steel bars (Ref-Steel). This is because the thermal bowing of the Ref-CFRP and PP-CFRP samples was restrained by the stiffness of the bars and their slightly negative longitudinal coefficient of thermal expansion (CTE) of approximately $-1.10^{-6}/°C$.

The longitudinal thermal contraction on heating, along with the higher modulus of elasticity of the CFRP bars, resists the elongation of the concrete sample – provided that bond slippage does not occur. The restraint force ceases to exist, however, once the CFRP bars slip within the surrounding concrete matrix. This effect can be clearly seen in Fig. 16 (for Ref-CFRP-C sample). By comparison, Fig. 17 suggests that the presence of the steel bars does not have the same restraining effect, and the sample is more free to thermally expand. This is due to the similarity in the coefficient of thermal expansion for both concrete and steel, as well as lower modulus of steel bars which allows a greater overall elongation than for the samples with CFRP bars.

Fig. 16 shows that the initial bowing (or out-of-plane displacement) for both Ref-CFRP-B and Ref-CFRP-C are identical (Ref-CFRP-B spalled, Ref-CFRP-C did not spall). However, the thermal bowing for Ref-CFRP-B deviated from Ref-CFRP-C at approximately-four minutes into the

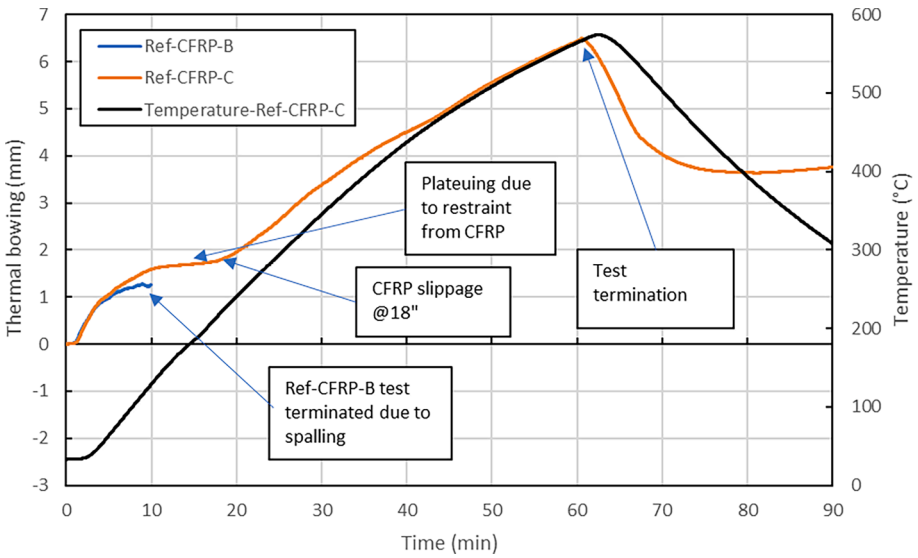

Fig. 16. Thermal Bowings Ref-CFRP-B compared to Ref-CFRP-C. The temperature–time history at the centre of the samples is also shown.

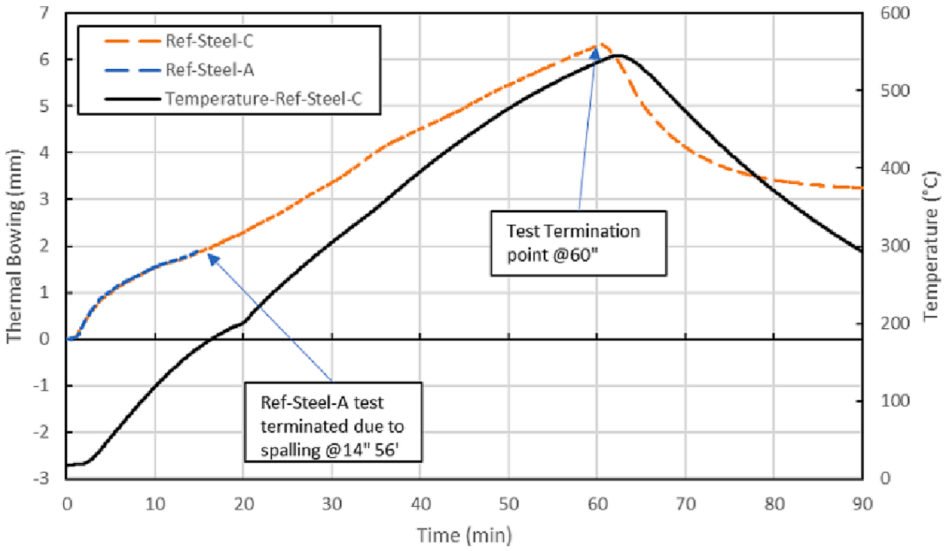

Fig. 17. Thermal Bowings Ref-Steel-A compared to Ref-Steel-C. The temperature–time history at the centre of the samples is also shown.

experiment. This was due the higher initial temperature at the centre of Ref-CFRP-C (30 °C), which led to an increased elongation (see Fig. 15). The thermal bowing of Ref-CFRP-C plateaued after the 10th minute due to the restraint from the CFRP bars mentioned earlier. However, the tendon's slippage at the 18th minute of the experiment (Ref-CFRP-C) led to an increased (and unrestrained) thermal bowing of the sample (6.42 mm after 60 min). This demonstrates the importance of the internal CFRP reinforcement in restraining thermal bowing.

Fig. 17 shows the thermal bowing of Ref-Steel-A and Ref-Steel-C. For Ref-Steel-A, the results are shown up to the 15th minute due to spalling occurring at that time. Fig. 17 shows that there is no obvious difference between Ref-Steel-A and Ref-Steel-C. Despite this, Ref-Steel-A spalled explosively at 14′56″ while Ref-Steel-C did not spall. For Ref-Steel-C, the maximum thermal bowing reached at 60 min was 6.31 mm (compared with 6.42 mm for CFRP above). No slippage or longitudinal cracks along the bars were recorded for any of the Ref-Steel samples. This demonstrates that the steel bars did not have the same restraining effect as the CFRP bars, due to their coefficient of thermal expansion being similar to concrete – as discussed previously.

The results of the thermal bowing for the PP-CFRP samples are shown in Fig. 18. The thermal bowing of specimens with PP fibres is less pronounced as compared with Ref-Steel samples. This is because the CFRP bars did not slip in this case (except for one of the two bars in Sample PP-CFRP-A), and thus the restraining effect of the bars remined in effect, therefore minimizing thermal bowing of all samples with PP fibres.

The results from the PP-CFRP and Ref-Steel samples provide further evidence that the restraining of the samples (against thermal bowing) appears not to be a controlling factor governing the occurrence of spalling.

As mentioned earlier, Sample PP-CFRP-A experienced slippage of one of its two bars at the 24th minute of the test. This led to a *partial* release of the restraint imposed by the CFRP bars. The results of this partial release (i.e., the extra out-of-plane movement) are visible in Fig. 18.

A comparison between the thermal bowing of the PP-CFRP samples and Ref-CFRP-B (up to the 10th minute) is shown in Fig. 19. This figure shows that the thermal bowing of Sample Ref-CFRP-B closely matched that of samples with PP fibres, even though Sample Ref-CFRP-B experienced multiple spalling events from the 6th minute up to the 10th

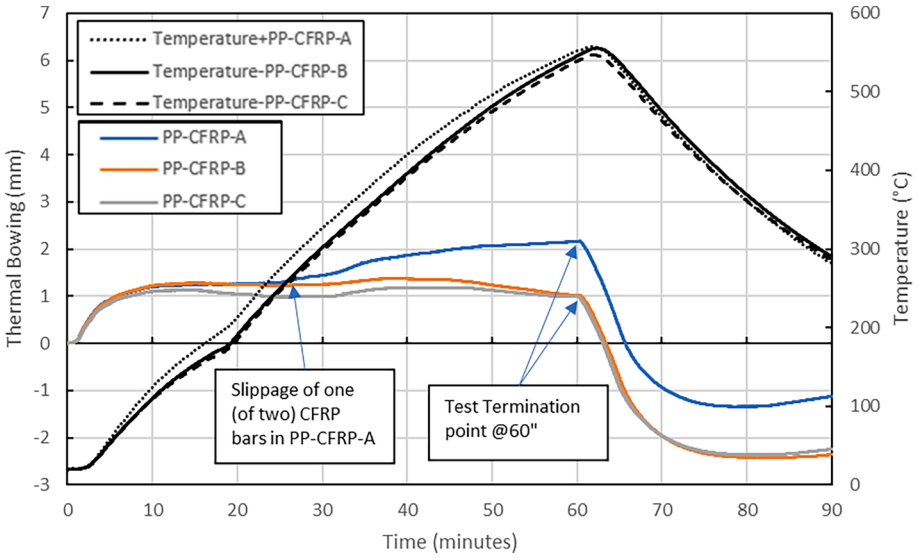

Fig. 18. Thermal bowing of PP-CFRP-A, PP-CFRP-B, and PP-CFRP-C samples against time. Temperature at the centre of each sample is shown.

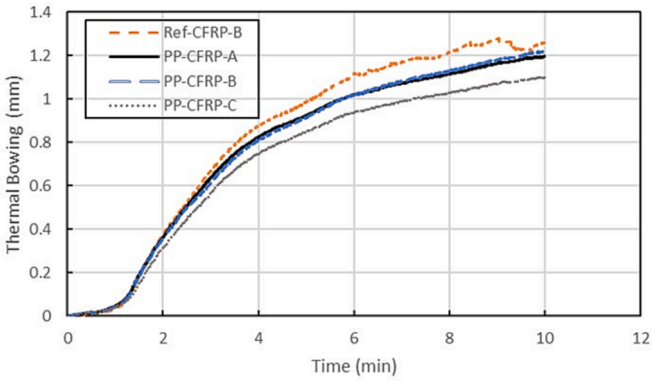

Fig. 19. Comparison of thermal bowing between samples Ref-CFRP-B, PP-CFRP-A and PP-CFRP-B.

minute (the PP-CFRP samples did not spall). This supports the hypothesis that the thermal bowing (which is a thermal stress release mechanism) appears not to be a governing factor for the occurrence of spalling; the presence of PP fibres is the critical factor.

3.5. The effects of moisture content

Moisture content was confirmed to play a central role in spalling. Samples Ref-CFRP-A and Ref-CFRP-B both spalled explosively, while Sample Ref-CFRP-C did not spall. All three samples had comparable levels of prestress (see Table 4) and had the same mix design and internal reinforcement. The only difference between the samples was the reduced level of moisture within Sample Ref-CFRP-C due to pre-drying. This result corroborates findings reported by Munguia [23], where concrete slabs exposed to an ISO 834 fire curve after pre-heating to 80 °C (for more than 30 days) avoided spalling altogether (similar samples that were not dried all spalled). Reduced internal moisture has been cited by other researchers as one of the main reasons behind samples avoiding spalling; Peng et al. [24] reported that combined curing led to higher degree of hydration, and by extension, lower levels of internal moisture. This effect, according to Peng, resulted in the samples with the lowest amount of internal moisture (referred to as free moisture by the author) to avoid spalling.

The experiments presented in this paper strongly point towards the moisture content as one of the main influencing factors for spalling. This was evident when comparing specimen Ref-CFRP-C to Ref-CFRP-B and Ref-CFRP-A. These results are being confirmed by further experiments.

It is noteworthy that some prestress may have been lost in Ref-CFRP-C during the drying due to shrinkage. This topic is currently being investigated.

3.6. The effect of prestress levels

The presence of compressive stress is shown in the literature to be (generally) adversely affecting the spalling likelihood of heated concrete samples [8,25]. Other researchers reporting that the direction (relative to crack formation) in which compressive stress is applied to be the main influencing factor [26] (i.e., when compressive stress is applied parallel to the cracks, it enhances permeability and reduces spalling, and vice versa). Nevertheless, the results from Ref-Steel samples indicate a lower likelihood of spalling with lower prestress levels, since the prestress in the Ref-Steel samples were on average 69 % less than the prestress levels in the Ref-CFRP samples (due to the lower modulus of elasticity of the steel bars). Further still, the prestressing within the Ref-Steel samples could have been reduced due to the deterioration of the elastic modulus of the steel bars with elevated temperatures. However, the results were not conclusive since one of the three Ref-Steel samples tested still spalled. Further experiments are needed to verify this hypothesis.

As mentioned earlier, it is possible that Ref-CFRP-C (pre-dried) lost some of its prestress during the drying process (due to shrinkage). It is possible that the potential reduced levels of prestress levels within this specimen helped it avoid spalling when subjected to a simulated ISO 834 fire curve. The reduction in prestress levels with oven drying also needs to be researched further.

The samples with PP fibres also had a reduced level of prestress (see Table 4). The reduced level of prestress could have played a part in the elimination of spalling for the PP-CFRP samples.

Overall, the likelihood of spalling was confirmed to be higher in samples with the highest levels of prestress. These findings are compatible with has been reported by a large number of researchers [26–30,31]. It is worth reiterating that compressive loading on its own may not be a factor that influences spalling; the real effect of loading is its influence on the further widening or closing cracks that facilitate the moisture transport, thus increasing or decreasing gas permeability at elevated temperatures. This effect has been demonstrated experimentally by Jihad et al. [26].

3.7. Formation of longitudinal cracks

In samples that did not spall, longitudinal splitting cracks were observed to form in samples with CFRP bars during the experiments. These cracks were not observed in samples with steel bars. The reason for the longitudinal cracking in CFRP prestressed samples is likely to be the larger transverse coefficient of thermal expansion (TCTE) of CFRP bars compared to the surrounding concrete. The temperature in the immediate surroundings of the CFRP bars at the time of the cracking is given in Table 5. The TCTE of CFRP is between three to eight times higher than that of concrete and steel, according to Aiello [32]. Some have even reported CTE (in the transverse direction) 8.4 times higher (at 150 °C) than concrete or steel [33]; and also reported the transverse expansion of the specific CFRP bars used in that work to be temperature dependent [33], as shown in Fig. 20.

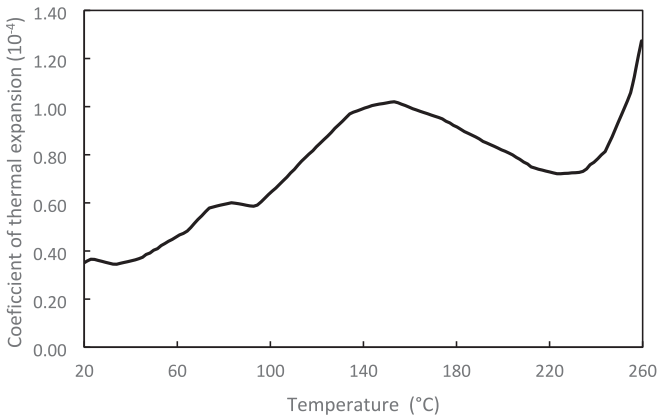

Fig. 20. Coefficient of thermal expansion (as a function of temperature) for CFRP bars used and reported in [33].

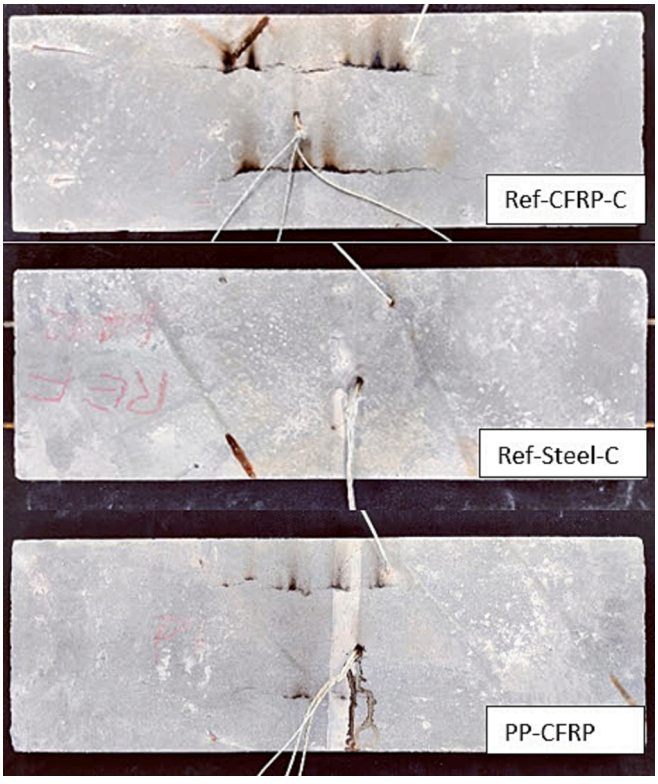

Fig. 21. The unexposed side of Ref-CFRP-C (top), Ref-Steel-C (middle), and PP-CFRP-C samples (bottom).

The transverse expansion of the CFRP bars is thought to cause the longitudinal cracks that were observed during the experiments. Fig. 21 shows the unexposed sides of non-spalled samples Ref-CFRP-C, Ref-Steel-C, and PP-CFRP-C; the longitudinal cracks can be observed in specimens with CFRP bars, while no cracks are visible in the specimen with steel reinforcement.

It is also noteworthy that longitudinal cracks observed in PP-CFRP samples appeared at a later stage than those in sample Ref-CFRP-C (see Table 5). This could be due to the effect of the PP fibres slowing down the crack propagation, as has been suggested in the literature [15,16].

4. Conclusions

The fire behaviour of self-prestressed planks is considered in this paper. Control mixes as well as modified mixes (with the addition of PP fibres) were prepared. Using a mobile gas-fired RPA, concrete planks were subjected to a simulated ISO 834 heating curve for a duration of one hour (or up until a 'main' spalling event). It can be concluded that:

1. Self-prestressed concrete planks are prone to explosive spalling when exposed to severe heating (similar to an ISO 834 standard heating exposure). Spalling occurred in less than 10 min for samples with CFRP bars, but no later than 15 min for any of the samples, when exposed to such conditions.
2. The higher levels of moisture content in the self-prestressed samples appears to be a governing factor for heat-induced spalling. When a specimen was dried until it lost more than half of its moisture content (Ref-CFRP-C), no spalling was observed, despite other (non-dried) samples within the same series all spalling in less than 9 min.
3. The addition of PP fibres to the concrete mix prevented spalling. 2 kg/m^3 of PP fibres led to the elimination of spalling in samples that were otherwise highly susceptible to spalling. This corroborates a wealth of available literature regarding the positive impacts of PP fibres on heat-induced explosive spalling in concrete.
4. The addition of PP fibres to the self-prestressed mixes reduced the level of self-prestressing by almost 30 %. Hypotheses have been advanced in this paper to explain this, but a lack of conclusive evidence means that no firm conclusions can be made regarding this observation at this stage.
5. A lower level of prestress appears to reduce the likelihood of spalling. Two out of three samples with 69 % less prestress levels (due to utilising steel bars instead of CFRP) avoided spalling under otherwise identical heating conditions.
6. Thermal stresses appear unlikely to be the governing factor in the spalling of self-prestressed concrete planks. It was observed that all samples with steel bars experienced considerable thermal bowing during the tests, but one of three samples still spalled, whilst very little thermal bowing was recorded for the PP-CFRP samples, none of which spalled.
7. In-depth temperature measurements confirm enhanced moisture migration within the concrete when PP fibres are used. It was observed that the PP-CFRP samples showed a markedly different in depth thermal response as compared with samples without PP fibres. This corroborates the role of PP fibres in facilitating an enhanced rate moisture transport and preventing the formation of a moisture clog within the concrete, thus mitigating heat-induced explosive concrete spalling.

5. Future work

Further experiments are necessary to understand the effects of the presence of pre-compressive stress (from prestressing) on spalling. The role of PP fibres in limiting the amount of expansion in self-prestressed concrete mixes also requires additional investigation. Further complimentary tests to thermally characterise the novel expansive concrete

mix are also needed, and will be performed in future work.

Declaration of Competing Interest

The authors declare that they have no known competing financial interests or personal relationships that could have appeared to influence the work reported in this paper.

Data availability

Data will be made available on request.

Acknowledgements

We would like to thank Dr Volha Semianiuk for the help with the initial mix design. We also acknowledge Mr Sebastiano Valvo, Mr Daniel Völki, Mr Christian Rohrer (Empa) for their assistance in the laboratory, alongside the efforts of Mark Partington and Michal Krajcovic from the University of Edinburgh.

References

[1] C.W. Dolan, H.R. Hamilton, Prestressed Concrete: Building, Design, and Construction. (2019).
[2] M. Wyrzykowski, G. Terrasi, P. Lura, Expansive high-performance concrete for chemical-prestress applications, Cem. Concr. Res., 107, February, pp. 275–283, 2018, doi: 10.1016/j.cemconres.2018.02.018.
[3] M. Wyrzykowski, G. Terrasi, P. Lura, Chemical prestressing of high-performance concrete reinforced with CFRP tendons, Compos. Struct., 239, December 2019, p. 112031, 2020, doi: 10.1016/j.compstruct.2020.112031.
[4] H. Mohammed, F. Sultangaliyeva, M. Wyrzykowski, G. Pietro Terrasi, and L. A. Bisby, "An Experimental Study into the Behaviour of Self-Prestressing, Self-Compacting Concrete at Elevated Temperatures," in 7th International Workshop on Concrete Spalling due to Fire Exposure, 12-14 October 2022, 2022, pp. 179–193, [Online]. Available: https://nbn-resolving.org/urn:nbn:de:kobv:b43-560798.
[5] J. Justs, M. Wyrzykowski, D. Bajare, P. Lura, Internal curing by superabsorbent polymers in ultra-high performance concrete, Cem. Concr. Res. 76 (2015) 82–90, https://doi.org/10.1016/j.cemconres.2015.05.005.
[6] H. Mohammed, H. Ahmed, R. Kurda, R. Alyousef, A.F. Deifalla, "Heat-Induced Spalling of Concrete: A Review of the Influencing Factors and Their Importance to the Phenomenon," Materials (Basel)., 15, 5, 2022, doi: 10.3390/ma15051693.
[7] G. Choe, G. Kim, M. Yoon, E. Hwang, J. Nam, N. Guncunski, Effect of moisture migration and water vapor pressure build-up with the heating rate on concrete spalling type, Cem. Concr. Res., 116, October 2018, 1–10, 2019, doi: 10.1016/j.cemconres.2018.10.021.
[8] P. Lura, G. Pietro Terrasi, Reduction of fire spalling in high-performance concrete by means of superabsorbent polymers and polypropylene fibers: Small scale fire tests of carbon fiber reinforced plastic-prestressed self-compacting concrete, Cem. Concr. Compos. 49 (2014) 36–42, https://doi.org/10.1016/j.cemconcomp.2014.02.001.
[9] C. Maluk, L. Bisby, M. Krajcovic, J.L. Torero, A heat-transfer rate inducing system (H-TRIS)test method, Fire Saf. J. 105 (2019) 307–319, https://doi.org/10.1016/j.firesaf.2016.05.001.
[10] I. Rickard, "Explosive Spalling of Concrete in Fire: Novel Experiments under Controlled Thermal and Mechanical Conditions," p. 390, 2020, [Online]. Available: https://era.ed.ac.uk/handle/1842/37473.
[11] H. Mohammed, D. Morrisset, A. Law, L. Bisby, "Quantification of the thermal environment surrounding radiant panel arrays used in fire experiments," in 12th Asia-Oceania Symposium on Fire Science and Technology (AOSFST 2021, 2021, no. December, pp. 7–9, doi: 10.14264/6efaa82.
[12] "Eurocode 2: Design of concrete structures. General rules - structural fire design," vol. 1, no. 2005, 2008.
[13] A. Carlton, Q. Guo, S. Ma, S. E. Quiel, and C. J. Naito, "Experimental assessment of explosive spalling in normal weight concrete panels under high intensity thermal exposure," Fire Saf. J., 134, August 2021, p. 103677, 2022, doi: 10.1016/j.firesaf.2022.103677.
[14] H. Mazaheripour, S. Ghanbarpour, S.H. Mirmoradi, I. Hosseinpour, The effect of polypropylene fibers on the properties of fresh and hardened lightweight self-compacting concrete, Constr. Build. Mater. 25 (1) (2011) 351–358, https://doi.org/10.1016/j.conbuildmat.2010.06.018.
[15] V. Afroughsabet, T. Ozbakkaloglu, Mechanical and durability properties of high-strength concrete containing steel and polypropylene fibers, Constr. Build. Mater. 94 (2015) 73–82, https://doi.org/10.1016/j.conbuildmat.2015.06.051.
[16] S. Fallah, M. Nematzadeh, Mechanical properties and durability of high-strength concrete containing macro-polymeric and polypropylene fibers with nano-silica and silica fume, Constr. Build. Mater. 132 (2017) 170–187, https://doi.org/10.1016/j.conbuildmat.2016.11.100.
[17] A. Sivakumar, M. Santhanam, Mechanical properties of high strength concrete reinforced with metallic and non-metallic fibres, Cem. Concr. Compos. 29 (8) (2007) 603–608, https://doi.org/10.1016/j.cemconcomp.2007.03.006.
[18] G. Terrasi, E.R.E. McIntyre, L.A. Bisby, T.D. Lämmlein, P. Lura, Transient thermal tensile behaviour of novel pitch-based ultra-high modulus CFRP tendons, Polymers (Basel) 8 (12) (2016) 10–20, https://doi.org/10.3390/polym8120446.
[19] Y.N. Chan, X. Luo, W. Sun, Compressive strength and pore structure of high-performance concrete after exposure to high temperature up to 800 °C, Cem. Concr. Res. 30 (2) (2000) 247–251, https://doi.org/10.1016/S0008-8846(99)00240-9.
[20] R.J. Mcnamee, "Fire Spalling – the Moisture Effect," 1st Int. Work. Concr. Spalling due to Fire Expo., no. September 2009, 2009.
[21] J. Bošnjak, J. Ožbolt, R. Hahn, Permeability measurement on high strength concrete without and with polypropylene fibers at elevated temperatures using a new test setup, Cem. Concr. Res. 53 (2013) 104–111, https://doi.org/10.1016/j.cemconres.2013.06.005.
[22] D. Zhang, A. Dasari, K.H. Tan, On the mechanism of prevention of explosive spalling in ultra-high performance concrete with polymer fibers, Cem. Concr. Res. 113 (August) (2018) 169–177, https://doi.org/10.1016/j.cemconres.2018.08.012.
[23] J.C. Mindeguia, P. Pimienta, H. Carré, C. La Borderie, Experimental analysis of concrete spalling due to fire exposure, Eur. J. Environ. Civ. Eng. 17 (6) (2013) 453–466, https://doi.org/10.1080/19648189.2013.786245.
[24] G.F. Peng, X.J. Niu, Y.J. Shang, D.P. Zhang, X.W. Chen, H. Ding, Combined curing as a novel approach to improve resistance of ultra-high performance concrete to explosive spalling under high temperature and its mechanical properties, Cem. Concr. Res. 109 (March) (2018) 147–158, https://doi.org/10.1016/j.cemconres.2018.04.011.
[25] C. Maluk, L. Bisby, G.P. Terrasi, Effects of polypropylene fibre type and dose on the propensity for heat-induced concrete spalling, Eng. Struct. 141 (2017) 584–595, https://doi.org/10.1016/j.engstruct.2017.03.058.
[26] M.J. Miah, H. Kallel, H. Carré, P. Pimienta, C. La Borderie, The effect of compressive loading on the residual gas permeability of concrete, Constr. Build. Mater. 217 (2019) 12–19, https://doi.org/10.1016/j.conbuildmat.2019.05.057.
[27] R. Jansson, L. Boström, Factors influencing fire spalling of self compacting concrete, Mater. Struct. Constr. 46 (10) (2013) 1683–1694, https://doi.org/10.1617/s11527-012-0007-z.
[28] J. Reiners, C. Müller, Einfluss der Zusammensetzung von Zementstein auf das Abplatzverhalten von Beton im Brandfall, Bautechnik 95 (8) (2018) 547–558, https://doi.org/10.1002/bate.201800031.
[29] H. Carré, P. Pimienta, C. La Borderie, F. Pereira, J.-C. Mindeguia, P. Pimienta, F. Meftah, Effect of compressive loading on the risk of spalling, MATEC Web Conf. 6 (2013) 01007.
[30] A. Behnood, M. Ghandehari, Comparison of compressive and splitting tensile strength of high-strength concrete with and without polypropylene fibers heated to high temperatures, Fire Saf. J. 44 (8) (2009) 1015–1022, https://doi.org/10.1016/j.firesaf.2009.07.001.
[31] L. Boström, U. Wickström, B. Adl-Zarrabi, Effect of specimen size and loading conditions on spalling of concrete, Fire Mater. 31 (3) (2007) 173–186, https://doi.org/10.1002/fam.931.
[32] M.A. Aiello, Concrete cover failure in FRP reinforced beams under thermal loading, J. Compos. Constr. 3 (1) (1999) 46–52.
[33] C. Maluk, "Development and Application of a Novel Test Method for Studying The Fire Baheviour of CFRP Prestressed Concrete Structural Elements," p. 473, 2014, [Online]. Available: http://hdl.handle.net/1842/16157.